

# Green Preparation of Carbon Dots for Intracellular pH Sensing and Multicolor Live Cell Imaging

*Wen-Jing Wang, Jun-Mei Xia, Ji Feng, Meng-Qi He, Ming-Li Chen\*, and Jian-Hua Wang\**

*Research Center for Analytical Sciences, Department of Chemistry, College of Sciences,*

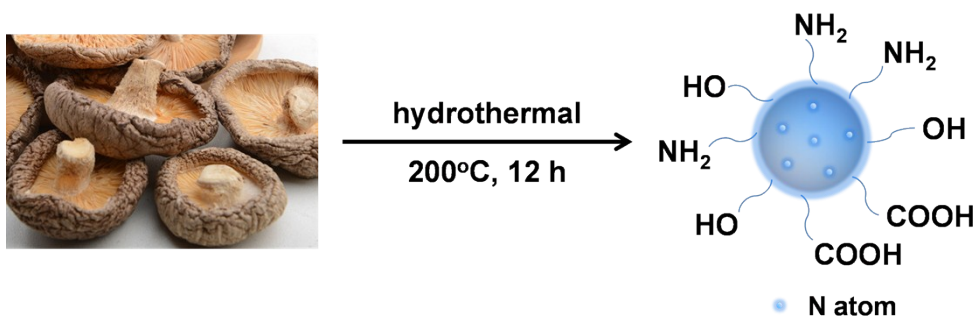
*Northeastern University, Box 332, Shenyang 110819, China*

**\*Corresponding author.**

E-mail address: chenml@mail.neu.edu.cn (M.-L. Chen), jianhuajrz@mail.neu.edu.cn

(J.-H. Wang).

Tel: +86 24 83688944; Fax: +86 24 83676698



Scheme S1 Schematic illustration for the preparation of MCDs.

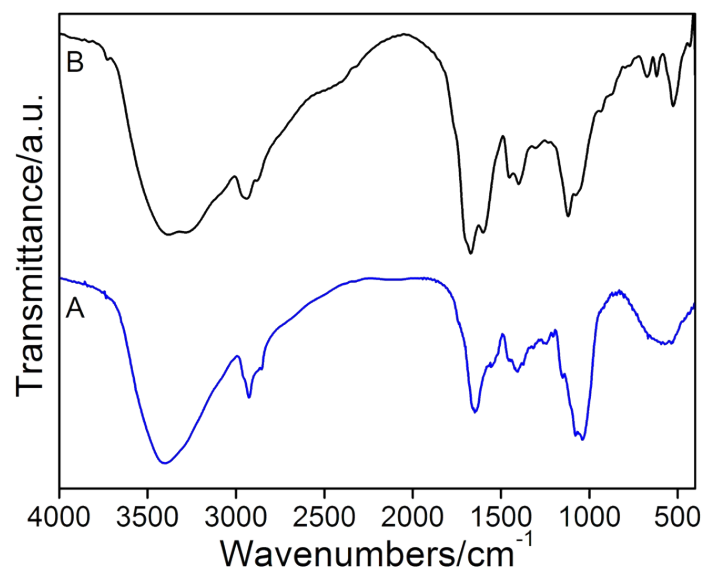


Fig. S1 FT-IR spectra of (A) the starting material (shiitake mushroom) and (B) the derived MCDs by following the preparation approach.

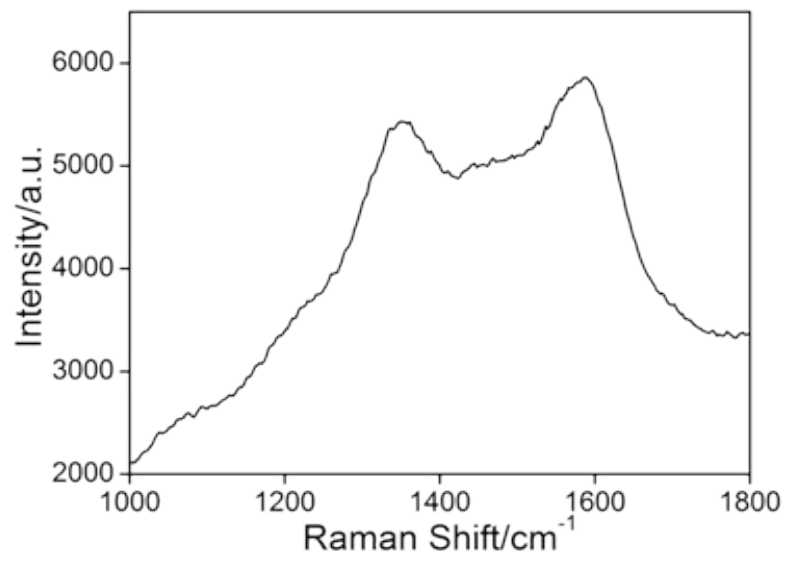


Fig. S2 Raman spectrum of the MCDs.

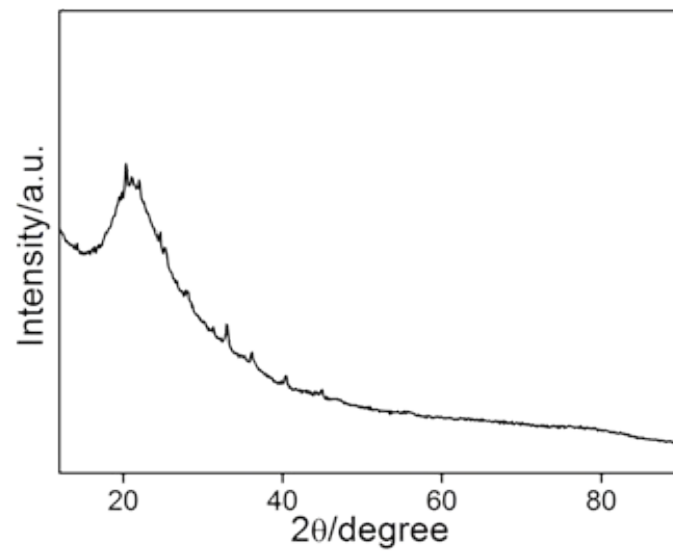


Fig. S3 XRD pattern of MCDs.

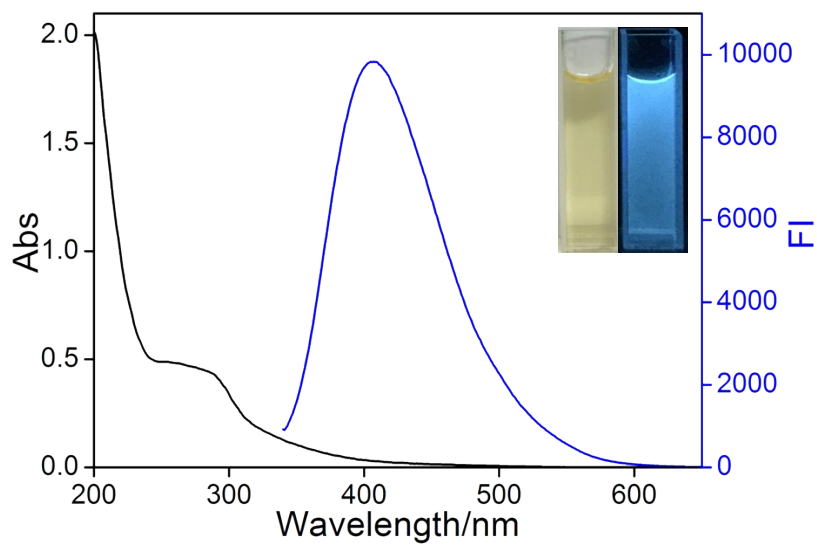


Fig. S4 UV-vis absorption spectrum and fluorescence emission spectrum of MCDs by excitation at 330 nm (Inset: MCDs solution irradiating under natural light (left) and UV light at 365 nm (right)).

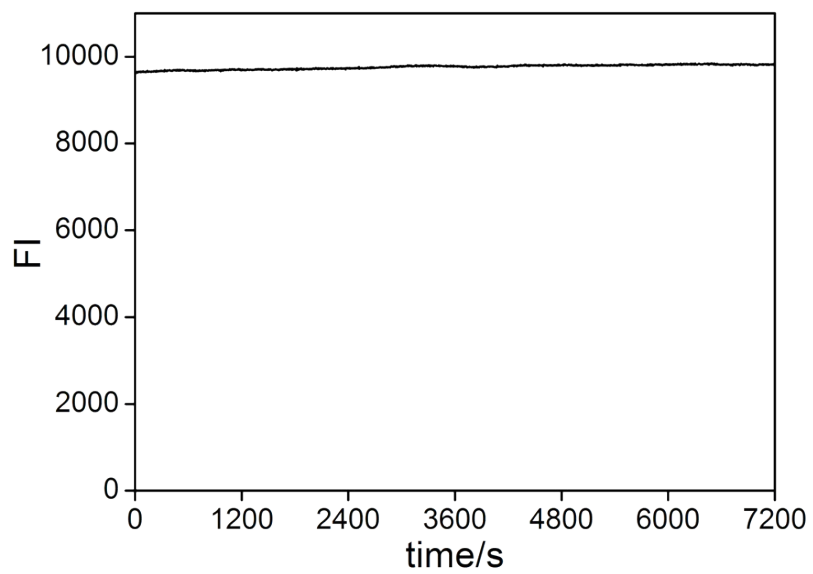


Fig. S5 The impact of irradiation time on the photoluminescence of MCDs.

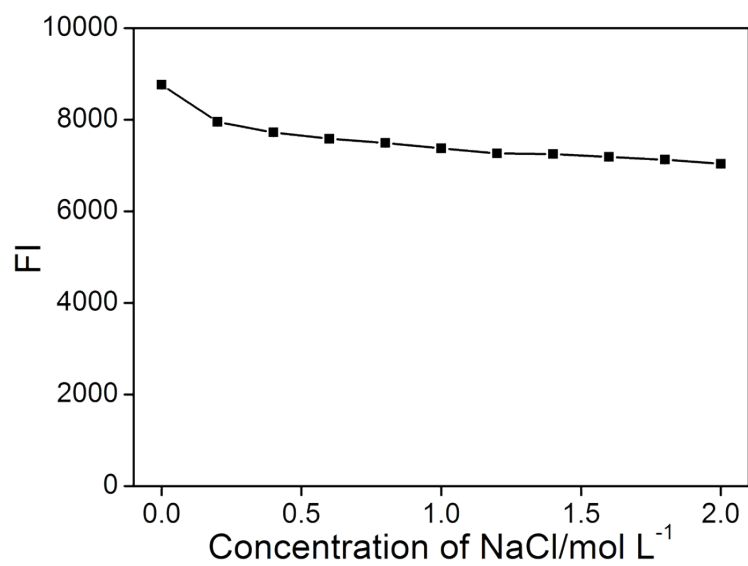


Fig. S6 The effect of ionic strength on the fluorescence intensity of MCDs.

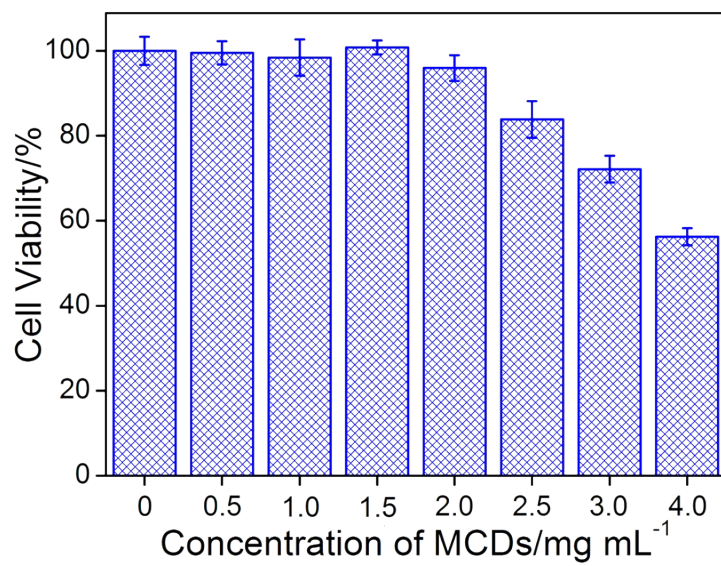


Fig. S7 The viability of HeLa cells after incubating with MCDs at various concentrations (from 0 to 4.0 mg mL<sup>-1</sup>).

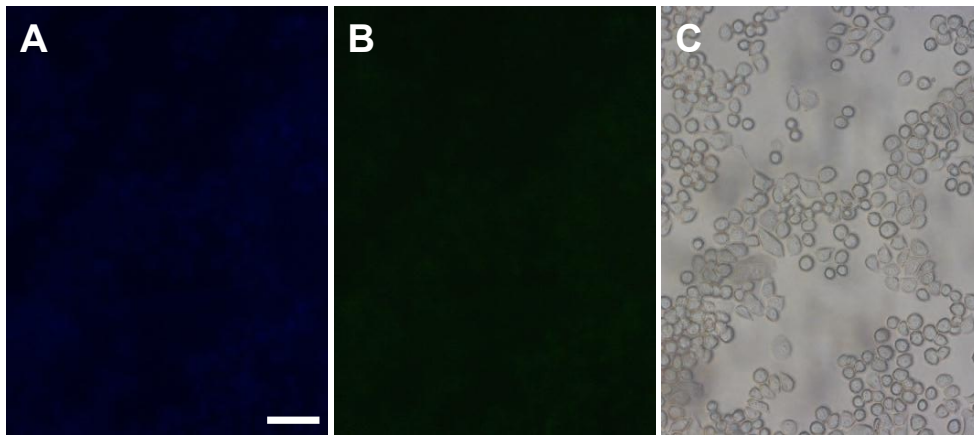


Fig. S8 The inverted fluorescence microscopic images of HeLa cells without labeling (A: with excitation at 340 nm; B: with excitation at 495 nm; C: bright field image. The scale bar stands for 100  $\mu\text{m}$ ).

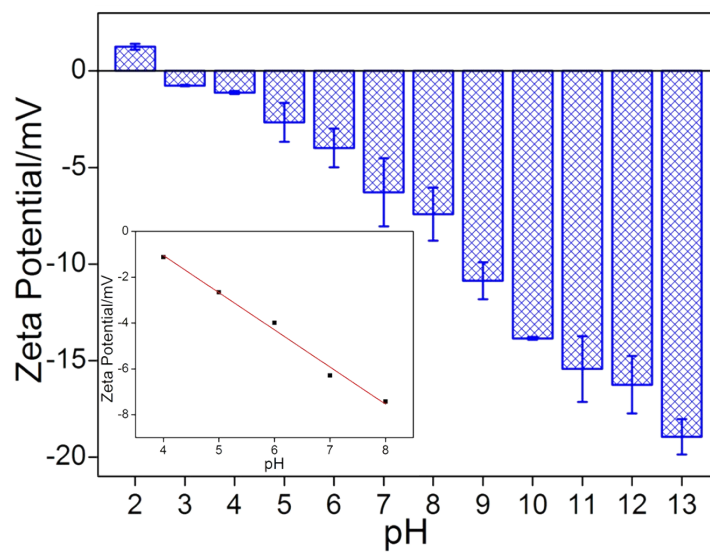


Fig. S9 Zeta potentials of MCDs in B-R buffer of different pH. Inset: the linear relationship between pH and zeta potential.

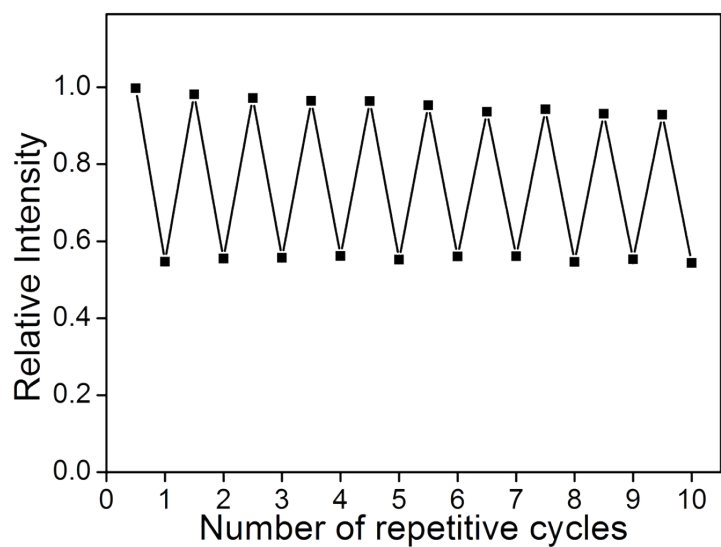


Fig. S10 The reversibility of the MCDs on the response to pH variation by regulating the pH value of the MCDs suspension from pH 2.0 to 13.0 and then adjusted back to 2.0 for 10 consecutive operation cycles.

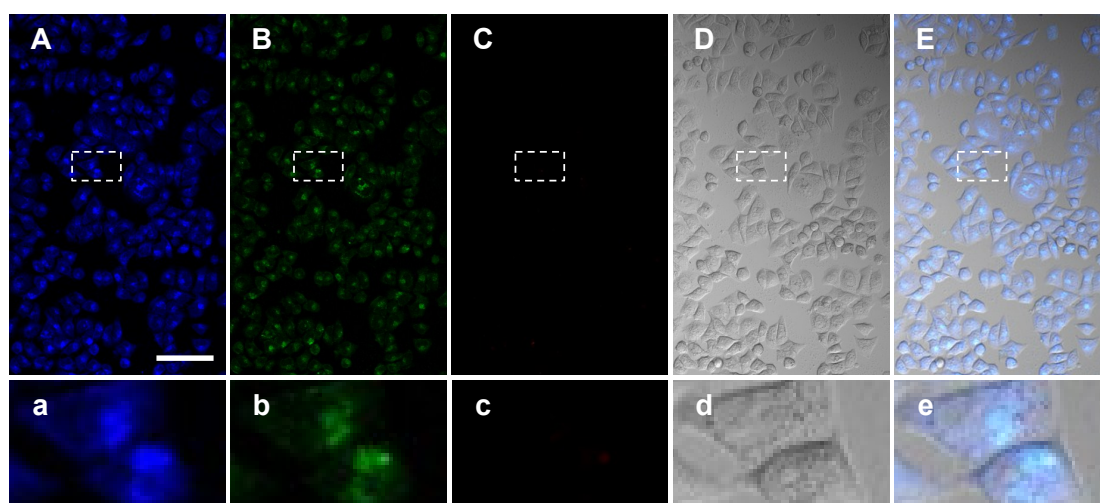


Fig. S11 The confocal fluorescence images of HeLa cells incubated with MCDs. The fluorescence images of (A), (B), (C) and (D) are collected in blue channel (420-480 nm,  $\lambda_{\text{ex}}$  405 nm), green channel (520-560 nm,  $\lambda_{\text{ex}}$  488 nm), red channel (575-655 nm,  $\lambda_{\text{ex}}$  561 nm) and bright field. (E) is the merge of (A), (B), (C) and (D). (a), (b), (c), (d) and (e) are the enlarged images of the chosen region. The scale bar stands for 100  $\mu\text{m}$ .

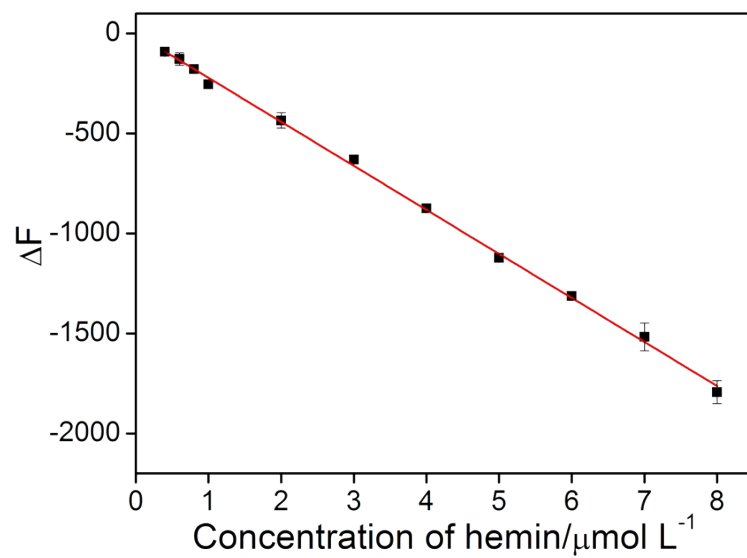


Fig. S12 The linear calibration graph between the net decrease of fluorescence intensity and the concentration of hemin.

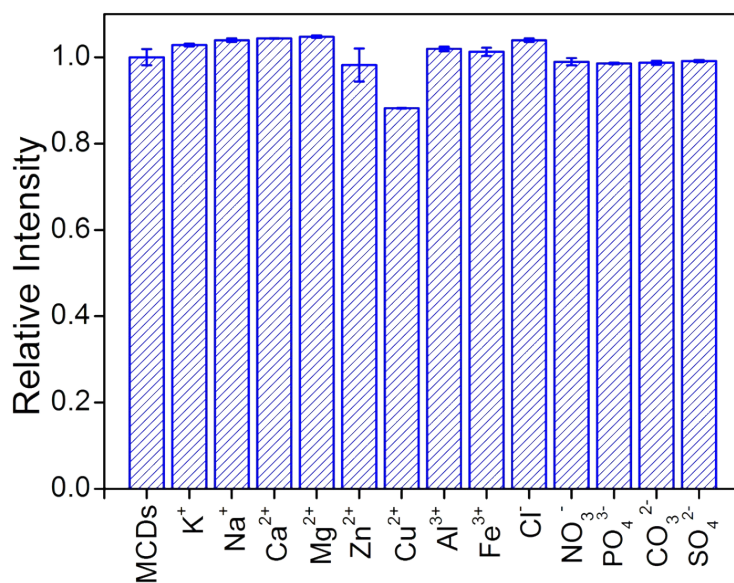


Fig. S13 The influence of different cationic and anionic species on the fluorescence of MCDs (the concentration of cation ions and anion ions: 1 mmol L<sup>-1</sup>).

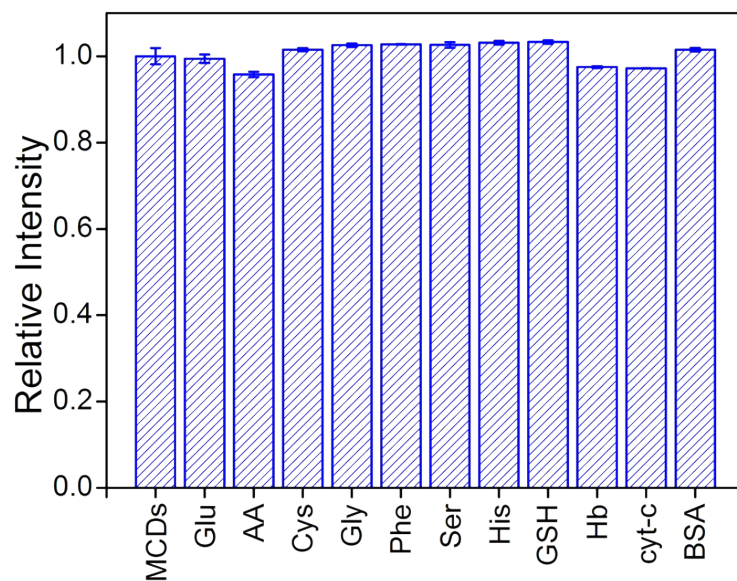


Fig. S14 The influence of different organic biological molecules on the fluorescence of MCDs (1 mg mL<sup>-1</sup> hemoglobin (Hb), cyt-c and bovine serum albumin (BSA), 1 mmol L<sup>-1</sup> glutamic acid (Glu), ascorbic acid (AA), l-cystein (Cys), glycine (Gly), phenylalanine (Phe), serine (Ser), histone (His) and glutathione (GSH)).

Table S1. Determination results for hemin in human serum, fetal bovine serum and hemin capsule by UV-vis absorption spectrophotometry and the present procedure (n=3, 95% confidence level).

Sample	UV-vis	This work
Human serum/g L <sup>-1</sup>	1.38±0.25	1.28±0.17
Fetal bovine serum/g L <sup>-1</sup>	1.33±0.30	1.41±0.04
Capsule/mg	58.93±10.51	55.87±0.03